Spring 5-15-2015

The C-terminal Linker of FtsZ Acts as an Intrinsically Disordered Peptide during Cell Division in Bacillus subtilis

Steven Grigsby
Washington University in St Louis

The C-terminal Linker of FtsZ Acts as an Intrinsically Disordered Peptide during Cell Division in *Bacillus subtilis*

By Steven Grigsby

Honors Thesis

Mentor: Dr. Petra Anne Levin

Washington University in St. Louis

Department of Biology

March 24, 2015

Abstract

The bacterial tubulin homologue FtsZ polymerizes *in vitro* in a GTP-dependent manner to form long, single stranded filaments. In cells, these filaments assemble at the nascent division site, interacting laterally to form the contractile Z ring. The Z ring serves as a scaffold for the rest of the division machinery and constricts at the leading edge of the invaginating septum during cytokinesis. The FtsZ polypeptide consists of three primary domains: the N-terminal globular core consisting of 315 residues that contains the GTP binding site, a variable and flexible C-terminal linker (CTL) consisting of 50 residues, and a conserved region at the C-terminus consisting of 17 residues required for interaction with modulatory proteins known as the grappling-hook peptide (GHP). Recently, the Levin lab has shown that the CTL behaves as a flexible intrinsically disordered peptide (IDP) and is required for FtsZ assembly *in vitro* and function *in vivo*.

To gain insight into the role the CTL in FtsZ assembly, together with our collaborators Rohit Pappu and Anu Mittal, I am testing the structural parameters that define a functional CTL. Using computational predictions developed by the Pappu lab, we have generated six CTL variants in the context of native FtsZ: CTLV1-CTLV6. By changing the order and patterning of charged residues in the IDP sequence, these variants undertake conformations ranging from linear to globular or hairpin-like structures. To characterize the impact of these variants on FtsZ ring formation *in vivo*, I am assessing their impact on Z ring formation, growth and division in the model bacterium *Bacillus subtilis*. My preliminary data suggest a range of CTL conformations is tolerated. However, significantly more flexible or more rigid linkers can lead to instabiltity and aberrant FtsZ assembly *in vivo*. Experiments performed with synthetic CTL linkers yield results that support this conclusion.

Chapter 1

A review of FtsZ and the Z-ring

Prokaryotic cell division is an exciting area of ongoing research. As in eukaryotes, cytoskeletal proteins play an important role in prokaryotic cell division. FtsZ is one such protein. First characterized by Bi and Lutkenhaus in 1991, at FtsZ polymerizes into a contractile ring at mid-cell that forms a scaffold for the division machinery, or divisome. (1). A suite of modulatory proteins regulate Z-ring assembly to coordinate it with the cell cycle (Figure 1) (35).

Figure 1. The bacterial division cycle. FtsZ assembly is coordinated with DNA replication and segregation. Step 1: In newborn cells FtsZ is unassembled. A circular chromosome with a single origin of replication is located at mid-cell. Steps 2–4: After chromosome replication initiates, the polymerase machinery remains at mid-cell, but origins of replication separate and move to opposite poles of the cell. Once replication is complete, the condensed chromosomes separate, leaving a nucleoid-free space. Step 3: Z-ring formation coincides with chromosome segregation. Assembly starts from a single point at mid-cell and extends bi-directionally. Step 5: During cytokinesis the Z-ring constricts at the leading edge of the invaginating septum. Small arrows indicate the assembly and disassembly of FtsZ subunits.

Essential for cell division, FtsZ is highly conserved across many divisions of bacteria and archaea and is also found in chloroplasts and mitochondria, which suggests an ancient origin for FtsZ that predates the eukaryotic cell. Due to the extensive homology between FtsZ and tubulin, it has been suggested that FtsZ, along with MreB, evolved into the eukaryotic cytoskeleton. Through evolution, however, new functions must have been acquired because FtsZ forms filaments that more closely resembles those of actin than tubulin (2). Interestingly, L-form
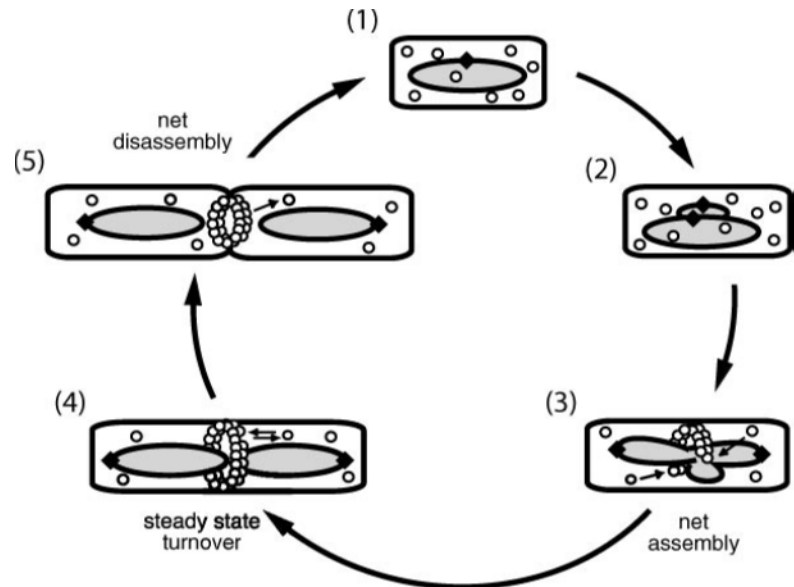
strains of bacteria that lack a cell wall are able to divide without FtsZ, which may suggest that

prokaryotic cells possessed ancestral division machinery before the evolution of a cell wall (3).

A series of recent studies has yielded tremendous insight into the structure of FtsZ (Figure 2) (33, 34). The data from these studies was used to construct a structural model of FtsZ containing three functional domains. At the N-terminus lies the widely conserved globular core, which bears the most homology to tubulin and contains the GTP-binding site. Until recently, the N-terminal globular core has been the most well characterized
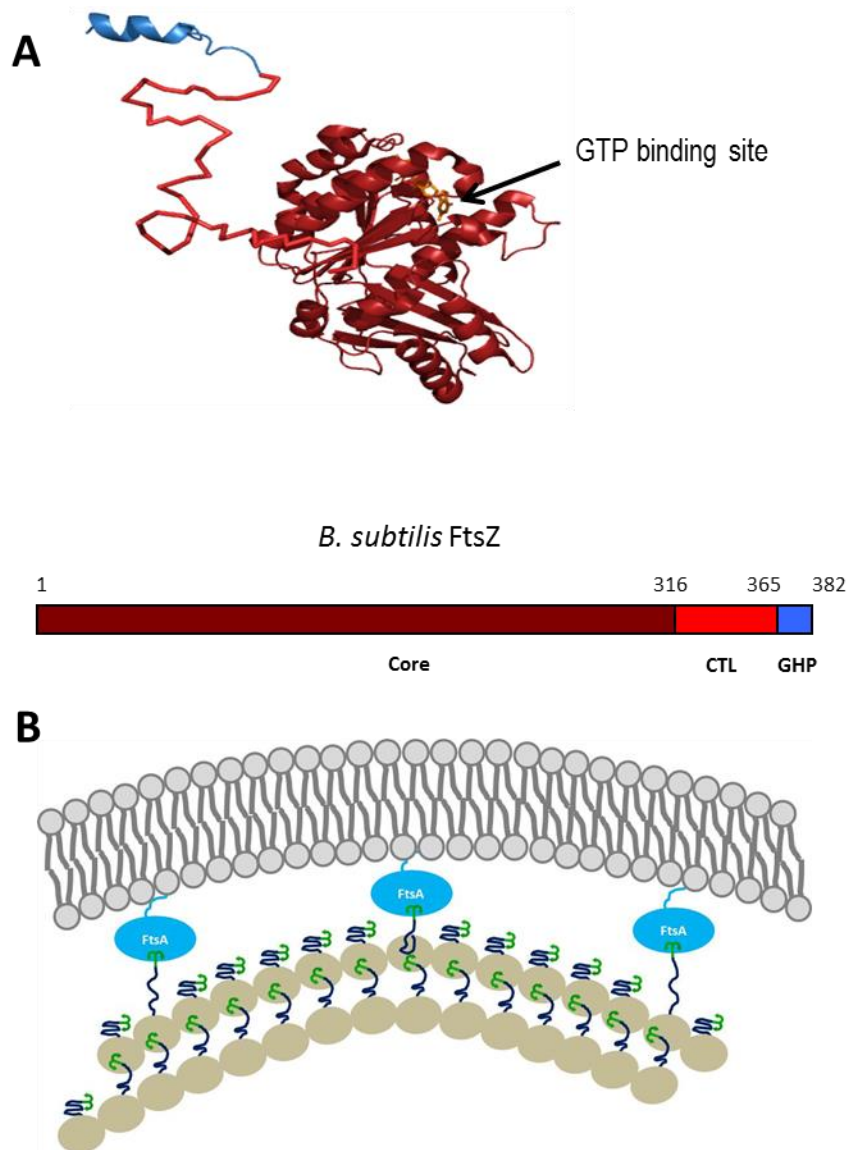
Figure 2. Structure of FtsZ and the Z-ring. A. FtsZ has three functional domains: the N-terminal globular core, the C-terminal linker (CTL), and the grappeling hook peptide (GHP). **B.** In the Z-ring, FtsZ protofilaments interact with other protofilaments and with FtsA, which anchors the Z-ring to the cell membrane, through the GHP.

domain. At the C-terminus lies a short sequence that has been designate the grappling hook

peptide (GHP) for its role in Z-ring assembly. The GHP contains binding site for modulatory

proteins and for lateral interactions between FtsZ polymers, without which Z-ring assembly fails and the cells form filaments. Part of the GHP is conserved, but the C-terminus is variable between species. Site-directed mutagenesis shows that the charge of the C-terminus is the primary determinant of lateral interaction potential, which explains differences between species observed *in vitro* (33). Between the core and GHP lies the C-terminal linker (CTL), an unstructured, highly variable domain, both in size and sequence, that remains the least understood (34).

The FtsZ ring, or Z-ring, serves as the backbone for assembly of the division machinery, or divisome. Using immunofluorescence microscopy, Levin and Losick found that the Z-ring is present in almost all cells, not just dividing ones, which means that the Z-ring assembles soon after division and remains assembled for most of the cell cycle until the next division (4). The source of the force necessary for cytokinesis, and FtsZ's contribution to it is unclear and an area of active research. FtsZ does not associate with any known motor proteins, but FtsZ has been found to provide its own constricting force in liposomes when an amphipathic helix is added to its C-terminus. This study also found that FtsZ can polymerize without the intervention of other proteins. The only other protein that is absolutely essential for cell division is FtsA, which binds to the C-terminus of FtsZ and anchors the Z-ring to the cell membrane via a C-terminal amphipathic helix (5). FtsZ and FtsA may be sufficient for division in liposomes, but the conditions are much different in live cells, which also have a cell wall that plays a role in cell division. In a study by Joseleau-Petit et al., L-form strains of *E.coli* still required peptidoglycan synthesis to grow and divide, which raises the possibility that the remodeling of the cell wall may provide a force pushing from without that closes the septum (6).

Similar to tubulin, FtsZ hydrolyzes GTP and acts as its own GAP. GTP hydrolysis proceeds at an appreciable rate only when FtsZ is assembled into a protofilament. The GTP hydrolysis active site is formed at the interface between two FtsZ monomers. The T7 synergy loop on the bottom interface of the FtsZ subunit, highly conserved in all FtsZ proteins, has been proposed to be the GAP that activates GTP hydrolysis in the GTP pocket of the subunit below (7). Unlike tubulin, FtsZ polymers contain a significant amount of GTP, indicating that there is a lag in GTP hydrolysis after polymerization. At steady state, 80% of the FtsZ subunits in a protofilament are bound to GTP. GTP hydrolysis, therefore, seems to be the rate-limiting step in GTP turnover, and FtsZ filaments may not possess the capability for dynamic instability that microtubules do. (8). GTP, however, is not necessary for FtsZ polymerization. Huecas and Andreu showed that apo-FtsZ from *Methanococcus jannaschii* can polymerize as efficiently as FtsZ-GTP, although adding GDP destabilizes the filaments (9). In fact, mutations in FtsZ that impair GTP hydrolysis but not binding can stabilize FtsZ polymers by reducing turnover of the subunits. The role of GTP, therefore, seems to be a means of destabilizing FtsZ filaments after hydrolysis, enabling the recycling of FtsZ subunits (10).

In vitro assays have revealed much information about the assembly dynamics of FtsZ (Figure 3) (35). The rate of protofilament turnover varies with the
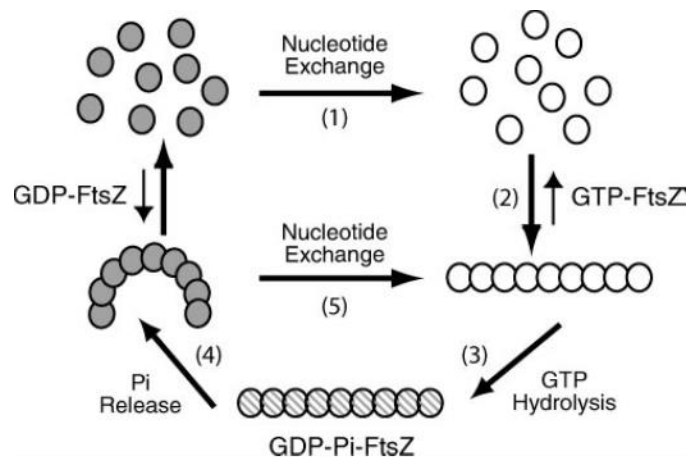
Figure 3. Model for FtsZ's GTP hydrolysis cycle. FtsZ's hydrolysis cycle is connected to polymer assembly and disassembly. 1: Monomers rapidly exchange nucleotide with solution. In vivo, more GTP than GDP exists in the cytoplasm. 2: When bound to GTP, FtsZ assembly is enhanced. 3: Once assembled, FtsZ can hydrolyze the GTP. 4: Phosphate release follows. GDP-containing polymers are more likely to be curved or to disassemble than GTP-containing polymers. 5: Nucleotide exchange might occur without complete disassembly of the polymer.

buffer conditions, varying from 3.5 to 35 seconds, but, the time for nearly full subunit exchange is generally equal to twice the time to hydrolyze one molecule of GTP, suggesting two mechanisms for subunit exchange in protofilaments: the exchange of one FtsZ subunit for every hydrolysis event and the exchange of FtsZ-GTP subunits at the filament ends without GTP hydrolysis (11). Once assembled, FtsZ protofilaments can assume two conformations: a straight one favored by GTP and a highly curved one favored by GDP. Those in the straight conformation tend to form sheets while those in the curved conformation tend to form minirings about 23 nm in diameter. For comparison, the diameter of the Z-ring is typically 500 nm – 1 µm. The transition from the straight conformation to the curved conformation provides a mechanism in which the energy of GTP hydrolysis is translated into a constricting force in the Z-ring (12). This data, along with the finding that Z-rings alone can constrict in liposomes, suggest that this step in the FtsZ assembly cycle accounts for at least part of the constricting force.

Under certain conditions that promote slower subunit exchange and GTP hydrolysis, lateral interactions between FtsZ protofilaments form, which drive the assembly of protofilaments into bundles. These higher-order structures begin to form when FtsZ reaches a concentration around 3 µM, higher than the critical concentration of 0.5 – 1 µM required for protofilament assembly (13). FtsZ protofilaments are generally around 100 nm long, much shorter than the circumference of the cell. A model of Z-ring substructure has been proposed in which the Z-ring is formed by short, overlapping protofilaments. Cryo-EM tomography data of Z-rings in *Caulobacter crescentus* supports this model (14). In most well-studied bacteria, the cellular concentration of FtsZ remains relatively constant throughout the cell cycle, about 3-10 µM in *E. coli*, with an average of 3200 molecules per cell (15). The regulation of FtsZ assembly,

therefore, lies not at the level of transcription, but in modulatory proteins that regulate the spatial organization, timing, and stability of FtsZ polymers.

The spatial regulation of FtsZ is governed by two distinct but overlapping systems. The first system prevents Z-ring assembly over the nucleoid through the action of DNA-binding proteins, Noc in *B. subtilis* and SlmA in *E. coli*. A possible mechanism for the inhibition of Z-ring assembly by SlmA was recently determined. Biochemical data shows that SlmA dramatically distorts DNA and binds as a dimer-of-dimers that can spread along the DNA. DNA-activates SlmA oligomerization would inhibit FtsZ polymerization and bundling. This system of nucleoid occlusion prevents Z-ring assembly before the replicating nuclei have segregated and also localizes the Z-ring to mid-cell between the segregated nuclei (16). The second system of spatial regulation consists of MinC, MinD, and MinE. MinD and MinE oscillate between the poles, creating a symmetric concentration gradient with a maximum at the poles and a minimum at mid-cell. MinC interacts with MinD through its C-terminal domain and FtsZ through its N-terminal domain. MinC couples the MinDE gradient to Z-ring assembly by inhibiting FtsZ polymerization at the poles, where the MinDE concentration is highest. As a result, the Z-ring does not assemble at the cell poles, preventing anucleate division. According to a recently proposed mechanism, MinC acts on FtsZ filaments in two ways: by increasing the detachment rate of FtsZ-GDP from the filaments and by reducing the attachment rate of FtsZ monomers to filaments by occupying binding sites on the FtsZ filament lattice. Data acquired from coreconstitution of FtsZ with MinCDE shows that the MinCDE system is sufficient for proper spatial regulation of Z-ring assembly (17). Together these systems ensure that the Z-ring forms only between segregating nuclei at mid-cell.

Another set of modulatory proteins regulate Z-ring assembly based on extracellular conditions. SulA is one such protein that is a negative regulator of Z-ring assembly in gammaproteobacteria. SulA is expressed during the SOS response to DNA damage and blocks cell division until the DNA is repaired, after which it is degraded. SulA inhibits both the GTPase activity and assembly of FtsZ. A recent study showed that SulA increases the critical concentration of FtsZ polymerization by binding competitively to FtsZ and sequestering it from polymerization. The increase in critical concentration is lower than the concentration of SulA, but the dissociation constants for FtsZ-FtsZ and FtsZ-SulA are very similar. SulA, therefore, establishes a competitive equilibrium between FtsZ binding to FtsZ or SulA (18). MciZ is another negative regulator of Z-ring assembly that is expressed during sporulation in *Bacillus* spp. The expression of MciZ is activated by the sporulation transcription factor Sigma E. *In vitro* data has shown that MciZ binds proximally to the GTP-binding site on FtsZ, inhibiting its GTPase activity and preventing polymerization (19).

There is also a set of proteins that couple cell division to nutrient conditions. Microbes have long been known to grow up to twice as large in nutrient-rich media as in nutrient-poor media. The glucolipid biosynthesis pathway acts as a nutrient sensor that modulates cell growth. PgcA, a phosphoglucomutase, catalyses the interconversion of glucose-6-phosphate, an intermediate of glycolysis, and glucose-1-phosphate, which can be converted to UDP-glucose by UTP-glucose-1-phosphate uridylyltransferase B (GtaB) and used in glycosylation reactions in biosynthesis. As a result, high glycolytic activity causes the concentration of UDP-glucose to rise. UgtP, an enzyme involved in synthesis of the diglucosyl-diacylglycerol anchor for lipoteichoic acid, the major anionic component of the Gram-positive cell wall, couples accumulation of its substrate UDP-glucose to cell division. In the presence of UDP-glucose,

UgtP binds to FtsZ and inhibits Z-ring assembly in high UDP-glucose conditions, thereby allowing cells to grow larger before dividing. Under low UDP-glucose conditions, UgtP oligomerizes and does not bind to FtsZ, which cause cells to be smaller when dividing (20).

Finally, there is a set of modulatory proteins that directly regulate Z-ring dynamics. ZapA is a widely conserved positive regulator of Z-ring assembly that increases Z-ring stability. *In vitro* 90° light scattering assays have shown that ZapA promotes the polymerization and bundling of FtsZ. *In vivo* microscopy experiments have shown that ZapA co-localizes with the Z-ring, forming a component of the division machinery. ZapA is not essential, but a ZapA:EzrA double knockout mutant is nonviable (21). EzrA is a negative regulator of Z-ring assembly that binds to the Z-ring and promotes depolymerization. Cells lacking EzrA have multiple rings at mid-cell and at the cell poles (22). Together, ZapA and EzrA contribute to Z-ring dynamics, without which the Z-ring is too static for cell division (23). SepF is another positive regulator of Z-ring assembly that forms rings *in vitro* ~50 nm in diameter, which are thought to bundle FtsZ protofilaments into a regular arrangement in the Z-ring. SepF mutants display deformed division septa, possibly due to a lack of order in the Z-ring (24).

FtsZ has long been recognized as an attractive potential target for antibiotics. Many natural products with antibacterial activity have been shown to inhibit FtsZ. GTP analogues have been shown to inhibit FtsZ polymerization *in vitro*. C8 MeOGTP inhibits FtsZ polymerization in *M. jannaschii* with an IC_{50} of 15 μM, and Compound 14 inhibits growth in *Staphylococcus aureus*. A family of compounds known as zantrins inhibits the GTPase activity of FtsZ. The most promising compound so far has been PC190723, which stabilizes FtsZ polymers and induces its association into large bundles (25). A study by Haydon et al. found that PC190723 provided 100% protection against a lethal dose of *S. aureus*. Several spontaneous mutation arose,

however, each consisting of a single amino acid change in FtsZ that conferred resistance in *S. aureus* (26). The use of FtsZ as an antibiotic target holds promise because of the effects it has on the cell. Cells depleted of FtsZ continue to grow and synthesize DNA for a few generations until they encounter a growth arrest, after which cells are unable to resume growth if FtsZ is reintroduced (27).

A review of intrinsically disordered peptides

Intrinsically disordered peptides (IDPs) are amino acid sequences that are unable to form a stable structure in solution. The disordered region of a protein can encompass the entire peptide sequence or just one domain, and the degree of disorder can range from molten globules to completely random coils. Due to a lack of structural constraints, IDPs care able to perform unique functions not readily fulfilled by canonically folding proteins: alternative splicing, movement through channels, post-translational modification, dual coding in alternative reading frames, and the creation of chimera proteins following gene fusion. IDPs with substantial net charge tend to assume extended conformations. IDPs with many charged residues but little or no net charge behave as polyampholytes, assuming extended conformations if the charges are randomly distributed and more compact conformations if the oppositely charged residues are more segregated. Neutral hydrophilic IDPs with few charged residues ten to form random collapsed structures to minimize contact with water. Hydrophobic IDPs tend to collapse into molten globules characterized by mobile side chains and unstable tertiary structures. Despite several known biological processes involving IDPs, they still remain relatively poorly characterized, but IDPs have recently exploded into a new field of active research with promising applications in medicine and biotechnology (28).

Polyampholytic IDPs are particularly interesting due to the range of available conformations, dependent on the distribution of oppositely charged residues. Due to this property, IDPs can display varying amounts of flexibility (Figure 4). The parameter κ
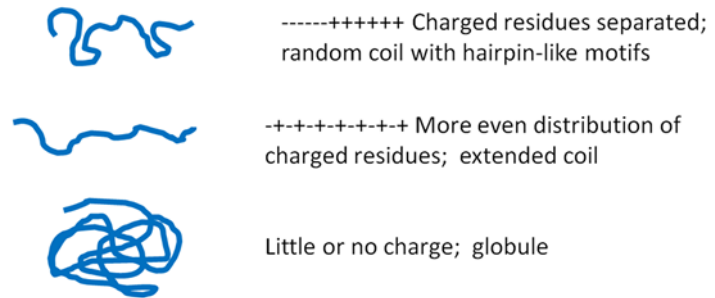

Figure 4. The effect of κ on polyampholytic IDP structure. The κ value of an IDP sequence is calculated as the relative separation of oppositely charged residues, which can influence which conformations are preferred.

was derived to measure this property. The value of κ lies on a scale from $0 - 1$. Low values of κ correspond to well-mixed sequences with even distribution of charged residues. In this peptide, attraction and repulsion are counterbalanced, causing the peptide to assume a loose random coil conformation. High values of κ correspond to sequences with opposite charges segregated, which tend to form compact hairpin-like conformations (29).

The C-terminal linker domain of FtsZ has been implicated as a polyampholytic IDP. The CTL displays a great amount of variation between species both in length, which can range from 2-330 residues, and sequence. Unlike the other domains, the structure of the CTL has not been resolved using x-ray crystallography, which suggests that the CTL lacks a well-defined structure. The CTL is essential for growth. Although the length of the CTL varies between species, sizeable deviations from the wild-type length are not tolerated within a species. Perhaps the most surprising finding is that the amino acid sequence of the CTL does not affect its function. As long as they are similar in length, CTLs can be exchanged between species without compromising function. This property of the CTL was confirmed when a scrambled CTL sequence conferred full functionality in *B. subtilis*. The CTL must also be unstructured for proper function. These findings have led to a model of FtsZ in which the CTL is a flexible tether that

allows lateral interactions between FtsZ filaments and with the cell membrane through the GHP. Consequently, its proposed role as a flexible tether is determined by the range of preferred conformations based on κ (34). Although the amino acid sequence of the CTL is not conserved, κ shows some conservation between species (29).

Many new discoveries have been made recently in the IDP field with the potential for impacts in medicine and biotechnology. The lack of an energetically defined stable structure makes IDPs particularly prone to misfolding and aggregation, which can then have pathological consequences. IDPs have been implicated in human disease, such as the microtubule-associated protein tau in Alzheimer's disease and α-synuclein in Parkinson's disease. Targeting these proteins with drugs has been challenging because of their poorly characterized heterogeneous conformational properties. A recent study, however, proposed a molecule that targets α-synuclein as a potential therapeutic for Parkinson's disease, showing that the targeting of these proteins is not only possible but treats some of the pathology caused by these proteins (30). Another recent study has shed some light on the regulation of the conformation and aggregation of IDPs, determining that urea promotes the aggregation of and that trimethylamine N-oxide promotes the formation of compact oligomers of tau. This finding suggest a possible role of osmolytes in the regulation of IDPs (31). Finally, the properties of IDPs allow for some unique biotechnological applications including, polypeptide nanoparticles for drug delivery, as solubilization tools, and as temperature-sensitive carriers of active peptides (32). The study of IDPs has far-reaching impacts in several areas of medicine, not only neurodegenerative but also infectious disease.

References

(1) Bi EF, Lutkenhaus J. FtsZ ring structure associated with division in *Escherichia coli*. Nature. 1991 Nov 14; 354 (6349): 161-4.

(2) Erickson HP. Evolution of the cytoskeleton. Bioessays. 2007 Jul; 29 (7): 668-77.

(3) Leaver M, Dominguez-Cuevas P, Coxhead JM, Daniel RA, Errington J. Life without a wall or division machine in *Bacillus subtilis*. Nature. 2009 Feb 12; 457 (7231): 849-53.

(4) Levin PA, Losick R. Transcription Factor Spo0A switches the localization of the cell division protein FtsZ from a medial to a bipolar pattern in *Bacillus subtilis*. Genes & Development. 1996 Feb 15; 10 (4): 478-88.

(5) Osawa M, Anderson DE, Erickson HP. Reconstitution of Contractile FtsZ Rings in Liposomes. Science. 2008 May 9; 320 (5877): 792-4.

(6) Joseleau-Petit D, Liebart JC, Ayala JA, D'Ari R. Unstable *Escherichia coli* L forms revisited: growth requires peptidoglycan synthesis. Journal of Bacteriology. 2007 Sep; 189 (18): 6512-20.

(7) Scheffers DJ, de Wit JG, den Blaauwen T, Driessen AJ. GTP hydrolysis of cell division protein FtsZ: evidence that the active site is formed by the association of monomers. Biochemistry. 2002 Jan 15; 41 (2): 521-9.

(8) Romberg L, Mitchison TJ. Rate-limiting guanosine 5'-triphosphate hydrolysis during nucleotide turnover by FtsZ, a prokaryotic tubulin homologue involved in bacterial cell division. Biochemistry. 2004 Jan 13; 43 (1): 282-8.

(9) Huecas S, Andreu JM. Polymerization of nucleotide-free, GDP- and GTP-bound cell division FtsZ: GDP makes the difference. FEBS Letters. 2004 Jul 2; 569 (1-3): 43-8.

(10) Anderson DE, Gueiros-Filho FJ, Erickson HP. Assembly dynamics of FtsZ rings in *Bacillus*

subtilis and *Escherichia coli* and effects of FtsZ-regulating proteins. Journal of

Bacteriology. 2004 Sep; 186 (17): 5775-81.

(11) Chen Y, Erickson HP. FtsZ filament dynamics at steady state: subunit exchange with and

without nucleotide hydrolysis. Biochemistry. 2009 Jul 21; 48 (28): 6664-73.

(12) Lu C, Reedy M, Erickson HP. Straight and curved conformations of FtsZ are regulated by

GTP hydrolysis. Journal of Bacteriology. 2000 Jan; 182 (1): 164-70.

(13) Esue O, Tseng Y, Wirtz D, The rapid onset of elasticity during the assembly of the bacterial

cell-division protein FtsZ. Biochemical and Biophysical Research Communications. 2005

Jul 29; 333 (2): 508-16.

(14) Li Z, Trimble MJ, Brun YV, Jensen GJ. The structure of FtsZ filaments *in vivo* suggests a

force-generating role in cell division. The EMBO Journal. 2007 Nov 14; 26 (22): 4694-

708.

(15) Rueda S, Vicente M, Mingorance J. Concentration and assembly of the division ring

proteins FtsZ, FtsA, and ZipA during the *Escherichia coli* cell cycle. Journal of

Bacteriology. 2003 Jun; 185 (11): 3344-51.

(16) Tonthat NK, Milam SL, Chinnam N, Whitfill T, Margolin W, Schumacher MA. SlmA

forms a higher-order structure on DNA that inhibits cytokinetic Z-ring formation over the

nucleoid. PNAS. 2013 Jun 25; 110 (26): 105896-91.

(17) Arumugam S, Petrasek Z, Schwille P. MinCDE exploits the dynamic nature of FtsZ

filaments for its spatial regulation. PNAS. 2014 Apr 1, 111 (13): E1192-200.

(18) Chen Y, Milam SL, Erickson HP. SulA inhibits assembly of FtsZ by a simple sequestration

mechanism. Biochemistry. 2012 Apr 10; 51 (14): 3100-9.

(19) Handler AA, Lim JE, Losick R. Peptide inhibitor of cytokinesis during sporulation in

Bacillus subtilis. Molecular Microbiology. 2008 May; 68 (3): 588-99.

(20) Weart RB, Lee AH, Chien AC, Haeusser DP, Hill NS, Levin PA. A metabolic sensor governing cell size in bacteria. Cell. 2007 Jul 27; 130 (2): 335-47.

(21) Gueiros-Filho FJ, Losick R. A widely conserved bacterial cell division protein that promotes assembly of the tubulin-like protein FtsZ. Genes & Development. 2002 Oct 1; 16 (19): 2544-56.

(22) Levin PA, Kurster IG, Grossman AD. Identification and characterization of a negative regulator of FtsZ ring formation in *Bacillus subtilis*. PNAS. 1999 Aug 17; 96 (17): 9642-7.

(23) Adams DW, Errington J. Bacterial cell division: assembly, maintenance and disassembly of the Z ring. Nature Reviews, Microbiology. 2009 Sep; 7 (9): 642-53.

(24) Gündoğdu ME, Kawai Y, Pavlendova N, Ogasawara N, Errington J, Scheffers DJ, Hamoen LW. Large ring polymers align FtsZ polymers for normal septum formation. The EMBO Journal. 2011 Feb 2; 30 (3): 617-26.

(25) Erickson HP, Anderson DE, Osawa M. FtsZ in bacterial cytokinesis: cytoskeleton and force generator all in on. MMBR. 2010 Dec; 74 (4): 504-28.

(26) Haydon DJ, Stokes NR, Ure R, Galbraith G, Bennett JM, Brown DR, Baker PJ, Barynin VV, Rice DW, Sedelnikova SE, Heal JR, Sheridan JM, Aiwale ST, Chauhan PK, Srivastava A, Taneja A, Collins I, Errington J, Czaplewski LG. An inhibitor of FtsZ with potent and selective anti-staphylococcal activity. Science. 2008 Sep 19; 321 (5896): 1673-5.

(27) Arjes HA, Kriel A, Sorto NA, Shaw JT, Wang JD, Levin PA. Failsafe mechanisms couple division and DNA replication in bacteria. Current Biology. 2014 Sep 22; 24 (18): 2149-

55.

(28) Oldfield CJ, Dunker AK. Intrinsically disordered proteins and intrinsically disordered protein regions. Annual Review of Biochemistry. 2014; 83: 553-84.

(29) Buske PJ, Mittal A, Pappu RV, Levin PA. An intrinsically disordered linker plays a critical role in bacterial cell division. Seminars in Cell & Developmental Biology. 2015 Jan; 37C: 3-10.

(30) Toth G, Gardai SJ, Zago W, Bertoncini CW, Cremades N, Roy SL, Tambe MA, Rochet JC, Galvagnion C, Skibinski G, Finkbeiner S, Bova M, Regnstrom K, Chiou SS, Johnston J, Callaway K, Anderson JP, Jobling MF, Buell AK, Yednock TA, Knowles TP, Vendruscolo M, Christodoulou J, Dobson CM, Schenk D, McConlogue L. Targeting the intrinsically disordered structural ensemble of α-synuclein by small molecules as a potential therapeutic strategy for Parkinson's disease. PLoS One. 2014 Feb 14; 9 (2): e87133.

(31) Levine ZA, LArini L, LaPointe NE, Feinstein SC, Shea JE. Regulation and aggregation of intrinsically disordered peptides. PNAS. 2015 Mar 3; 112 (9): 2758-63.

(32) Uversky VN. Proteins without unique 3D structures: Biotechnological applications of intrinsically unstable/disordered proteins. Biotechnology Journal. 2014 Oct 6.

(33) Buske PJ, Levin PA. Extreme C terminus of bacterial cytoskeletal protein FtsZ plays fundamental role in assembly independent of modulatory proteins. Journal of Biological Chemistry. 2012 Mar 30; 287 (14): 10945-57.

(34) Buske PJ, Levin PA. A flexible C-terminal linker is required for proper FtsZ assembly *in vitro* and cytokinetic ring formation *in vivo*. Molecular Microbiology. 2013 Jul; 89 (2): 249-63.

(35) Romberg L, Levin PA. Assembly dynamics of the bacterial cell division proteins FtsZ: poised at the edge of instability. Annual Review of Microbiology. 2003; 57: 125-54.

Chapter 2

Introduction

FtsZ is a bacterial homologue of tubulin that assembles into a contractile ring at mid-cell, which serves as a scaffold for the rest of the division machinery (1). FtsZ is widely conserved across many divisions of bacteria (2). A series of recent studies has yielded tremendous insight into the structure of FtsZ. The data from these studies was used to construct a structural model of FtsZ containing three functional domains. At the N-terminus lies the widely conserved globular core, which bears the most homology to tubulin and contains the GTP-binding site. At the C-terminus lies a short sequence that has been designate the grappling hook peptide (GHP) for its role in Z-ring assembly. The GHP contains binding site for modulatory proteins and for lateral interactions between FtsZ polymers. Part of the GHP is conserved, but the C-terminus is variable between species (9). Between the core and GHP lies the C-terminal linker (CTL), an unstructured, highly variable domain, both in size and sequence, that remains the least understood (10).

The domain between the core and GHP, the C-terminal linker (CTL), remains the least understood domain of FtsZ and is the focus of this study. The CTL, similarly to the C-terminus, displays a great amount of variation between species both in length, which can range from 2-330 residues, and sequence. Unlike the other domains, the structure of the CTL has not been resolved using x-ray crystallography, which suggests that the CTL lacks a well-defined structure. A previous *in vivo* study of the CTL examined strains expressing FtsZ chimeras, containing the wild-type core and GHP and a variant CTL sequence, yielded some insight into the function of the CTL. Although the length of the CTL varies between species, sizeable deviations from the wild-type length are not tolerated within a species. Perhaps the most surprising finding is that the

amino acid sequence of the CTL does not affect its function. As long as they are similar in length, CTLs can be exchanged between species without compromising function. This property of the CTL was confirmed when a scrambled CTL sequence conferred full functionality in *B. subtilis*. These findings have led to a model of FtsZ in which the CTL is a flexible tether that allows lateral interactions between FtsZ filaments and with the cell membrane through the GHP (10).

These properties of the CTL are typical of an intrinsically disordered peptide. In this study, I examined the effects that the expression of FtsZ chimeras have on cell division *in vivo*. Similar to the previous study, these chimeras contain CTL variant sequences designed using mathematical modelling (Figure 1) .The native CTL variants were designed by changing the order of residues in the wild-type *B. subtilis* CTL so that the amino acid content of the wild type CTL is conserved. The synthetic CTL variants were designed using only five amino acids, and the amino acid content of the wild type CTL is not conserved. These variants were designed to lie on a range of κ values, which refers to the distribution of oppositely charged residues, close to that of wild type and on either extreme of the spectrum. Together, these variants will allow the determination of the role of the κ value of the CTL and its characterization as an IDP.

Methods

General methods and growing conditions

Cells were grown in Luria-Bertani (LB) medium at 37°C. Antibiotics were used at the following concentrations: ampicillin = 100 μg/mL, spectinomycin = 100 μg/mL, chloroamphenicol = 5 μg/mL. The strains expressing CTL variant FtsZ, derived from PAL 2084, were grown in 0.5% xylose to induce wild-type expression or 0.1 mM IPTG to induce CTL variant expression. Vent DNA polymerase was used for PCR (New England Biolabs). All

restriction enzymes were ordered from New England Biolabs. All genomic DNA extractions

were done using the Wizard Genomic DNA Purification Kit (Promega). Plasmid preps were

done using the NucleoSpin Plasmid Kit (Macherey-Negel). Gel/PCR purifications were done

using the NucleoSpin Gel and PCR Clean-up Kit (Macherey-Negel). T4 DNA ligase was used

for ligations (New England Biolabs).

ID	Sequence	L	FCR	|NCPR|	κ
WT BS	IEQEKDVTKPQRPSLNQSIKTHNQSVPKREPKREEPQQQNTVSRHTSQPADDTLDIPTFLRNRNKRG	67	0.33	0.06	0.19
CTLV1	GSHQPKPEQKSEANQSREQVTRELHSRNVPEIQKKDKVPQQPSTNTSTPQRIPGDDTLDIPTFLRNRNKRG	71	0.31	0.06	0.15
CTLV2	GSVQNKQIEKQKEPERRQRTHVESSPHQPSSQPVDRNPLPKTNQTQEKASITPGDDTLDIPTFLRNRNKRG	71	0.31	0.06	0.18
CTLV3	GSHQKPRQKVNKRQSEIRVPQSELSRSPTQENEEQSQPPAKTKNVQDTIHTPPGDDTLDIPTFLRNRNKRG	71	0.31	0.06	0.34
CTLV4	GSHPPEQQISKTRKRHVTQSQQEDEPPAKQKSLRRQNQEINVVNSSKPETTPPGDDTLDIPTFLRNRNKRG	71	0.31	0.06	0.4
CTLV5	GSPQIHQPKPQKKRSSNPTDQHKSAVTTPRKRVLIRQQPQTESEVEEESNQNPGDDTLDIPTFLRNRNKRG	71	0.31	0.06	0.46
CTLV6	GSNSQTQIRKRRKKKKRSSHQIVNLPNAPPDPEEEESEPHQSQTQPTVTQVQPGDDTLDIPTFLRNRNKRG	71	0.31	0.06	0.72
S_WT	GSPRQSEEPSRVVSEPSSQPRHQRQEVRERPHRRQQQEVSAVVSQQSSQPQRPGDDTLDIPTFLRNRNKRG	71	0.31	0.06	0.21
S_V1	GSERERSQQHESPQSSQSRVHQPQPVPVRSAEQVPQRVVEQPSSQQRSRERRPGDDTLDIPTFLRNRNKRG	71	0.31	0.06	0.17
S_V5	GSSQHSPAEQVQEEEESVSSSPHPRRRSQQRVPEPQQPQRVRRSRVVQRSQQPGDDTLDIPTFLRNRNKRG	71	0.31	0.06	0.47

Figure 1. FtsZ Variant Sequences. The CTL sequences of every CTL Variant used in this study is shown here. Uncharged residues are shown in black, positively-charged residues are shown in blue, and negatively-charged residues are shown in red. Green residues are the translation of restriction site added to the ends of the CTL to facilitate cloning. The GHP is shown in purple. The CTL Variants were designed exhibit a range of κ values: some similar to that of wild type, some with a higher κ, and some with a lower κ. L=length. FCR=fraction of charged residues. NCPR=net charge per residue.

Designing CTL variant sequences

The sequences of the CTL variants were designed using the parameter κ, calculated using

a mathematical modelling program described previously (7). Briefly, the parameter κ represents

the distribution of oppositely charged residues in an IDP. Other important parameters used in the

designing of the CTL variant sequences are net charge per residue (NCPR) and the fraction of

charged residues (FCR). The native CTL variants were designed by changing the order of

residues in the wild type *B. subtilis* linker, keeping the amino acid content of wild type

conserved. The variants were designed to include the conserved range of κ values seen in wild

type populations, as well as some outliers in the high- and low-κ range not seen in wild type to

test the effect of these extreme κ values. The synthetic CTL variants were designed synthetically

to match the κ values of the native CTL variants, which does not conserve the amino acid content

of the wild type CTL.

Strain or Plasmid	Genotype/features	Source
B. subtilis		
JH642	*trpC2 pheA1*	Ref 12
PAL 2084	JHC642 *thrC::P_{xyl}-ftsZ*	Ref 11
PAL 3171	PAL 2084 *amyE::P_{spac}-ftsZ*	Ref 9
PAL 3491	PAL 2084 *amyE::P_{spac}-ftsZCTLV1*	This study
PAL 3495	PAL 2084 *amyE::P_{spac}-ftsZCTLV2*	This study
PAL 3499	PAL 2084 *amyE::P_{spac}-ftsZCTLV3*	This study
PAL 3503	PAL 2084 *amyE::P_{spac}-ftsZCTLV4*	This study
PAL 3507	PAL 2084 *amyE::P_{spac}-ftsZCTLV5*	This study
PAL 3511	PAL 2084 *amyE::P_{spac}-ftsZCTLV6*	This study
PAL 3639	PAL 2084 *amyE::P_{spac}-ftsZCTLSV1*	This study
PAL 3643	PAL 2084 *amyE::P_{spac}-ftsZCTLSV5*	This study
PAL 3663	PAL 2084 *amyE::P_{spac}-ftsZCTLSWT*	This study
E. coli		
AG1111	*DZR200- MC1061 F'lacIQ lacZM15 Tn10 (tet)*	Ref 13
PAL 930	AG1111 + pBS58	Ref 11
Plasmids		
pPJ19	pET21b(+)-*ftsZ946-51 BamHI 1090-95 XmaI* stop	Ref 10
pPJ53	pET21b(+)-*ftsZCTLV1* stop	This study
pPJ54	pDR67-*ftsZCTLV1* stop	This study
pPJ55	pET21b(+)-*ftsZCTLV2* stop	This study
pPJ56	pDR67-*ftsZCTLV2* stop	This study
pPJ57	pET21b(+)-*ftsZCTLV3* stop	This study
pPJ58	pDR67-*ftsZCTLV3* stop	This study
pPJ59	pET21b(+)-*ftsZCTLV4* stop	This study
pPJ60	pDR67-*ftsZCTLV4* stop	This study
pPJ61	pET21b(+)-*ftsZCTLV5* stop	This study
pPJ62	pDR67-*ftsZCTLV5* stop	This study
pPJ63	pET21b(+)-*ftsZCTLV6* stop	This study
pPJ64	pDR67-*ftsZCTLV6* stop	This study
pSG1	pET21b(+)-*ftsZCTLSV1* stop	This study
pSG2	pDR67-*ftsZCTLSV1* stop	This study
pSG3	pET21b(+)-*ftsZCTLSV5* stop	This study
pSG4	pDR67-*ftsZCTLSV5* stop	This study
pSG5	pET21b(+)-*ftsZCTLSWT* stop	This study
pSG6	pDR67-*ftsZCTLSWT* stop	This study

Table 1. Bacterial strains and plasmids used in this study.

Cloning CTL variants

The CTL variant strains were constructed as described previously with some

modifications (10). The bacterial strains and plasmids used in this study are listed in Table 1.

Synthetic double-stranded oligonucleotides of the CTL variants were ordered from Integrated

DNA Technologies, restriction digested, and ligated into pPJ19, which contains *ftsZ*, under the

control of the P_{spac} promoter inducible with 0.1 mM IPTG, with restriction sites flanking the

CTL. A *Bam*HI site after aa 315 and a *Xma*I site before aa 366 result in the aa pairs GS and PG

upstream and downstream of the CTL, respectively. The plasmid was transformed into PAL 644,

a strain of *E. coli* derived from PL930. PAL 644 contains the low copy plasmid pBS58

expressing *E. coli ftsQAZ*, which allows the sub-cloning of *B. subtilis ftsZ*. *FtsZ* was amplified in

pPJ19, the product of which was restriction digested, purified, and ligated into pDR67. The

multiple cloning site in the vector pDR67 contains the 5'- and 3'-ends of the *amyE* gene on

either side, which allows the insertion of *ftsZ* into the *amyE* locus by homologous recombination.

The purified plasmid was transformed into PAL 522, a derivative of the JH642 wild-type strain

of *B. subtilis*. Genomic DNA was purified and transformed into MEO 1, a derivative of PAL

2084 containing a copy of wild-type *ftsZ* under the control of the P_{xyl} promoter, inducible with

0.5% xylose. The cells were made competent and transformed with purified genomic DNA from

PAL 2084, which knocks out the chromosomal wild-type copy of *ftsZ*. Plasmids were verified by

restriction digests and sequencing.

Immunoblotting

Immunoblotting was performed as described previously (11). Cells were grown overnight

in 0.5% xylose, back-diluted 1:100 and grown in 0.5% xylose until the cells reached mid-log

phase. The cells were then washed twice with LB, diluted 1:100, and grown to mid-log phase in

0.1 mM IPTG. The cells were lysed with lysozyme and detergent. Loading was normalized to the

OD_{600} at sampling. The blot was probed using affinity-purified polyclonal rabbit anti-FtsZ

antibodies (3) and goat anti-rabbit antibodies conjugated to horseradish peroxidase (Jackson

ImmunoResearch Laboratories). Immunoblots were developed using the ECL Western Blotting detection reagents (GE Healthcare) and visualized with the luminescent image analyzer ImageQuant LAS 4000 mini (GE Healthcare).

Growth Curves

Cells were grown overnight in 0.5% xylose, back-diluted 1:100 and grown in 0.5% xylose until the cells reached mid-log phase. The cells were then washed twice with LB, diluted to OD_{600} 0.004, and grown in 0.1 mM IPTG. Starting 1 hour after induction, the OD_{600} was measured every 30 minutes for 4 hours.

Immunofluorescence microscopy

Immunofluorescence microscopy was performed as described previously (9). Cells were grown overnight in 0.5% xylose, back-diluted 1:100 and grown in 0.5% xylose until the cells reached mid-log phase. The cells were then washed twice with LB, diluted 1:100, and grown in 0.1 mM IPTG for 5 generations (~2.5 hours). The cells were harvested and fixed with 16% paraformaldehyde/0.5% gluteraldehyde. The cells were lysed with 2 mg/mL lysozyme. FtsZ was detected with affinity-purified polyclonal rabbit anti-FtsZ serum (3) in combination with goat anti-rabbit serum conjugated to Alexa488 (Life Technologies). Cell walls were stained with wheatgerm agglutinin conjugated to tetramethylrhodamine, and DNA was stained with DAPI. Slides were visualized with an Olympus BX51 microscope with Chroma filters and a Hamamatsu OrcaERG camera and processed using Openlab version 5.2.2 (Improvision) and Adobe Photoshop CS version 8.0 (Adobe Systems).

Measuring cell length/Z-ring ratio

The cell length/Z-ring (L/R) ratio was calculated as described previously (4). The L/R ratio was calculated as the sum total cell length of a population of cells divided by the total number of Z-rings in that population.

Results

CTL Variants with extreme κ values do not support growth

It was determined in the previous study that cells expressing CTL variant FtsZ can be viable (10). This was also the case in this study. Figure 5 shows that several strains expressing CTL variant FtsZ grow at the same rate as wild type. CTL6, the highest κ variant, exhibits growth for ~5 generations and then encounters

Figure 2. Growth Curve of Native CTL Variants. CTL variants with a κ value close to that of wild type grow at the normal rate. CTLV5, a high-κ variant, exhibits an immediate growth arrest after induction. CTLV6, the highest-κ variant, exhibits a delayed growth arrest similar to that of an FtsZ knockout strain.

a growth arrest, after which cells begin to die. This pattern of growth resembles that of an FtsZ knockout strain (6), which suggests that CTLV6 is nonfunctional. The high κ value of CTLV6 was predicted to render it insoluble, which would account for its lack of functionality. CTLV5 has a slightly lower κ value than CTLV6 but, unlike CTLV6, exhibits an almost immediate growth arrest, suggesting that CTLV5 is directly toxic to the cells. The incorporation of CTLV5
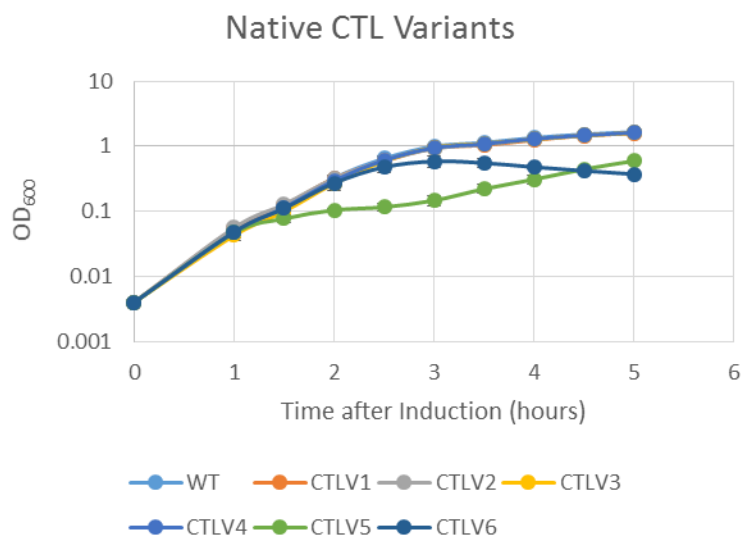
into the Z-ring may be poisoning it and making it unstable. The later increase in growth may be due to spontaneous suppressor mutants that are able to express wild type FtsZ again.

<p style="text-align:center">*CTL variants with extreme κ values are degraded by the cells*</p>

An immunoblot analysis of the native CTL variants showed that extreme-κ variants are present in low levels in the cells (Figu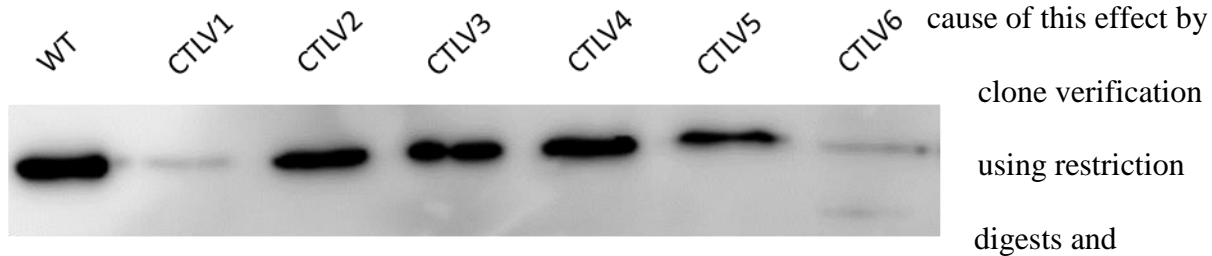re 6). Lower expression of these variants was ruled out as a cause of this effect by clone verification using restriction digests and sequencing.

Figure 3. Immunoblot of Native CTL Variants. The CTL variants with κ values close to that of wild type are tolerated by the cells. FtsZs with extreme κ values are degraded by the cells.

Sequencing at the vector-insert junctions shows that the constructs are cloned correctly and should be expressed at the same level as wild type. It was, therefore, determined that the cells are actively degrading these variants, which suggests that they may not be well tolerated by the cells. CTL variants with a κ value closer to that of wild type seem to be well tolerated by the cells, and are present in the cell at the same level as wild type.

<p style="text-align:center">*Cells expressing CTL variants with extreme κ values are longer and have fewer Z-rings*</p>

Imaging the cells with immunofluorescence microscopy shows the same overall trend in the native CTL variants (Figure 7). FtsZs that form unstable Z-rings cause the cells to grow longer than wild type. The L/R ratio serves as a proxy for cell length, with wild type at ~6 – 7 μm. CTLV6 has very few Z-rings and instead has FtsZ localized in granules. Consequently, the cells form long filaments. The DAPI staining shows cells in distress with a loss of nucleoid structure. CTLV5 exhibits a mix of long, filamentous cells with no Z-rings and short cells with Z-rings that appear similar to wild type. The short cells are likely suppressor mutants expressing

wild type FtsZ. Many of the filamentous cells expressing CTLV5 appear to be lysed, further evidence of its toxicity to the cells. Interestingly, CTLV1, which grows at the same rate as wild type, has longer cells with a greater L/R ratio than wild type. CTLV1 may confer just enough functionality to FtsZ so that the cells can still double in mass at the normal rate, but is still less functional than wild type.
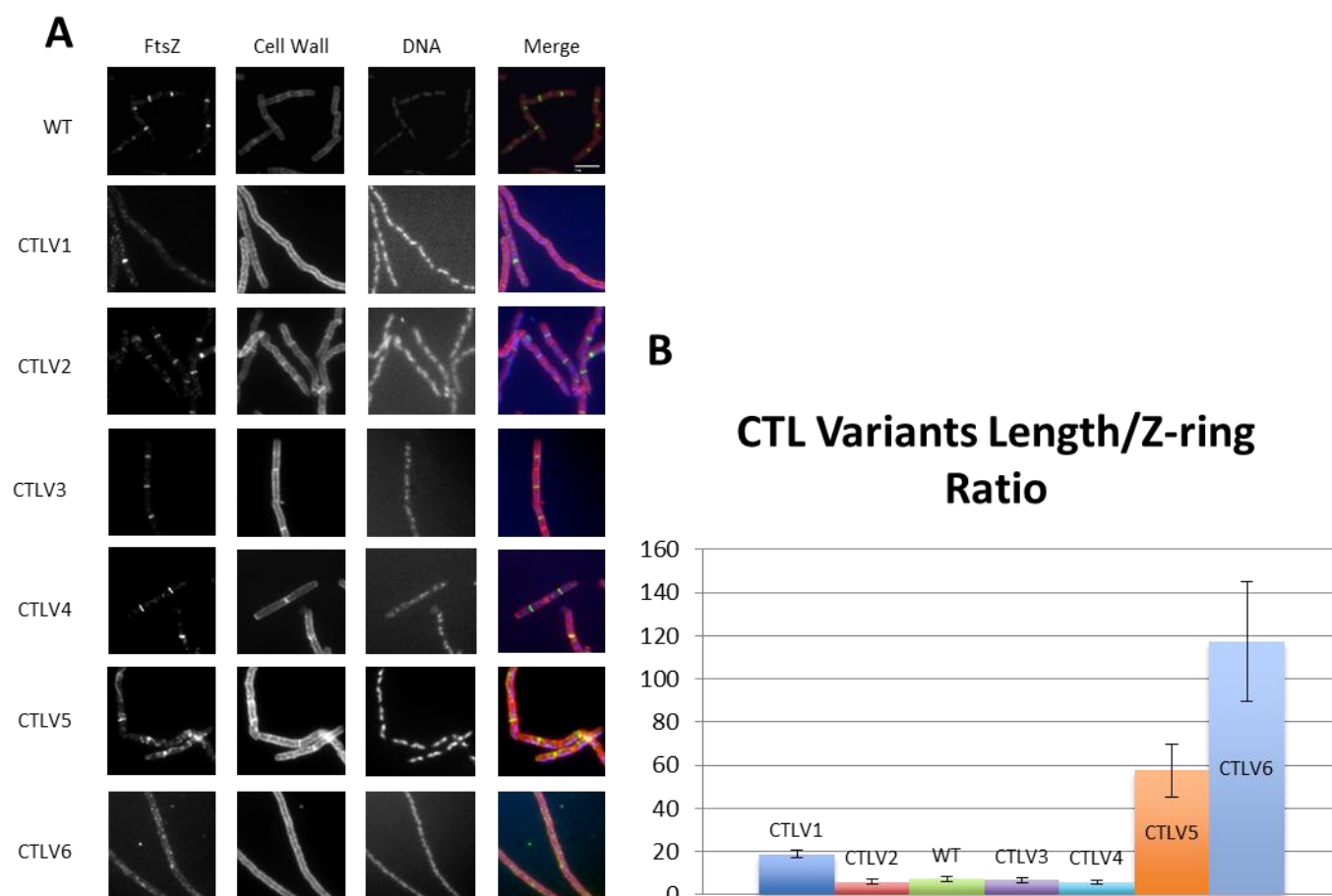

Figure 4. Immunofluorescence microscopy of the native CTL Variants. A. Cells expressing FtsZs with extreme κ values appear longer and have fewer Z-rings than wild type. B. Cells expressing FtsZ with extreme κ values have greater L/R ratios than wild type.

CTLV5 is a dominant negative mutation

Co-expression of native CTL variant and wild type FtsZ is able to rescue the growth of some variant strains (Figure 8). The rescue of the growth of cells expressing CTLV6 by co-expression of native CTL variant and wild type FtsZ provides additional evidence that CTLV6 is
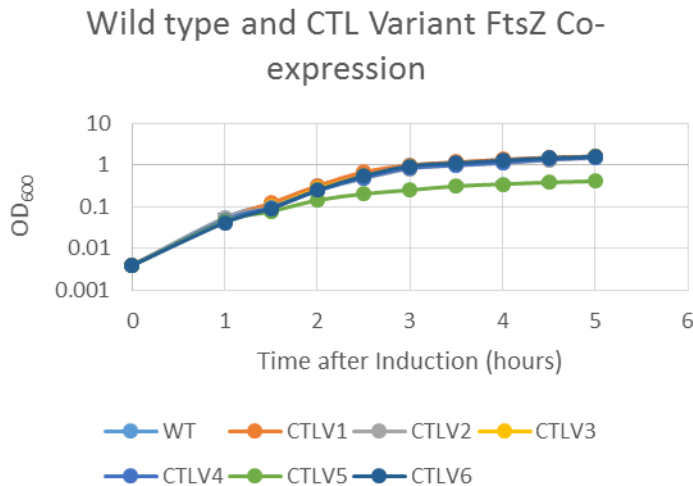
Wild type and CTL Variant FtsZ Co-expression

Figure 5. Growth curve of co-expressed wild type and native CTL Variant FtsZ. CTLV5 is a dominant negative mutation. Co-expression of wild type and CTL variant FtsZ rescues growth in all variants except CTLV5.

nonfunctional and does not interact with wild type FtsZ. CTLV5, however, is a dominant negative mutation because co-expression of native CTL variant and wild type FtsZ is unable to fully rescue growth. This result supports the model of Z-ring assembly in which the incorporation of CTLV5 monomers into an otherwise wild type Z-ring poisons the entire structure, thus rendering the cells unable to divide. The immediate growth arrest and toxicity seen with CTLV5, which are not seen with CTLV6, suggest that CTLV5 is having additional effects in the cell through an unknown mechanism.

Synthetic CTL variants exhibit the same dependence on κ as the native CTL variants

Synthetic CTL variants exhibit the same overall pattern in growth and viability with regards to κ. CTLSWT, which has the same κ as wild type grows at almost the same rate as wild type, although slightly slower. CTLSV1 and CTLSV5, which have the same κ as CTLV1 and CTLV5, respectively, fail to grow altogether in a manner similar to an FtsZ knockout strain, suggesting that these variants are nonfunctional. All synthetic CTL variants are degraded in the cells, although CTLSWT is degraded to a much less degree than CTLSV1 and CTLSV5. Using immunofluorescence microscopy, the cells expressing CTLSWT appear similar to wild type, with a similar L/R ratio. CTLSV1 and CTLSV5 appear similar to CTLV5: filamentous cells with very few Z-rings.
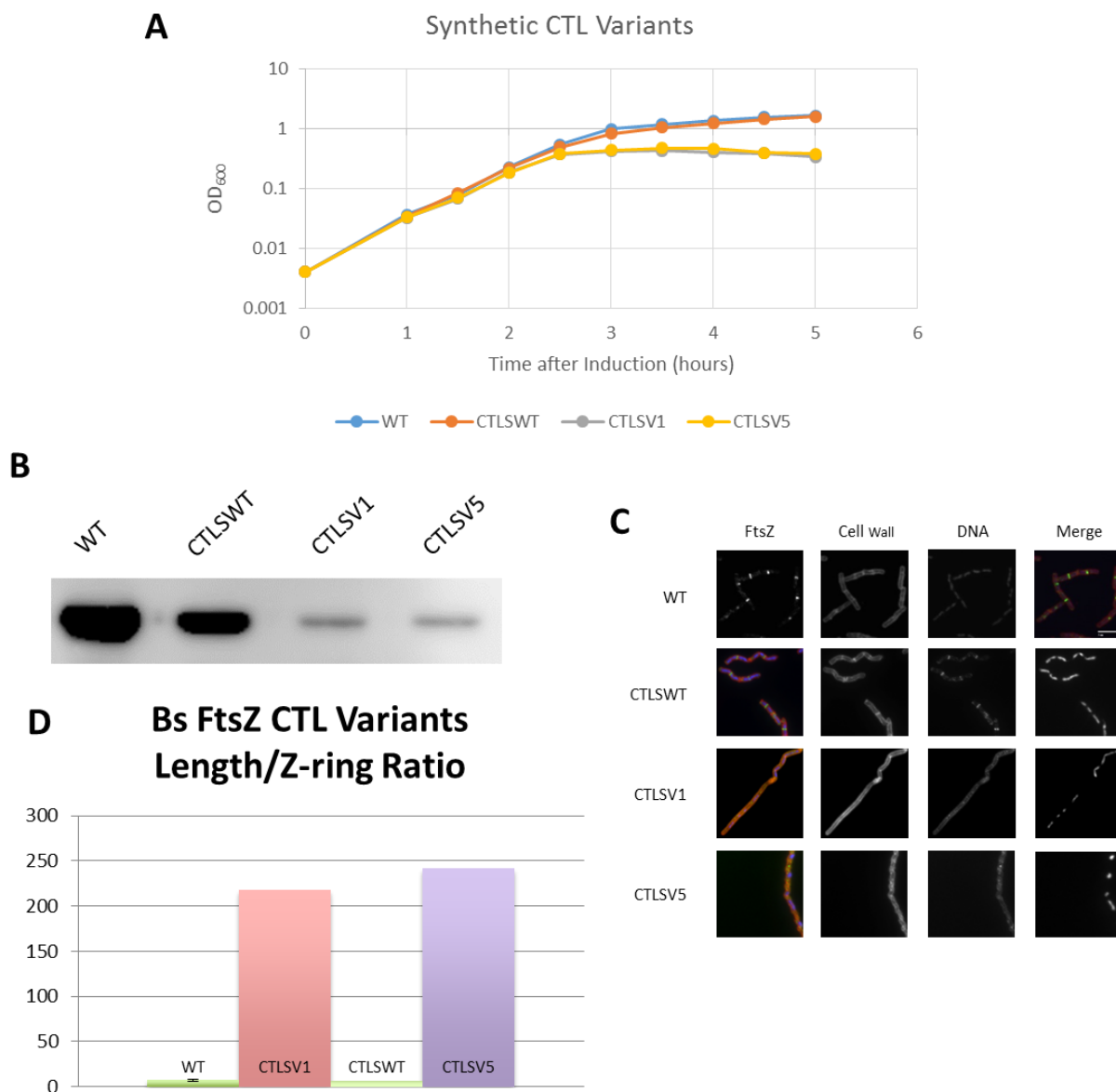
Figure 6. Synthetic CTL Variants exhibit the same dependence on κ for growth as the native CTL Variants. A. CTLSWT grows at about the same rate as wild type. CTLSV1 and CTLSV5 exhibit a growth arrest similar to that of an FtsZ knockout. B. The synthetic CTL Variants are degraded *in vivo*, especially CTLSV1 and CTLSV5. C. Cells expressing CTLSWT appear similar to wild type. Cells expressing CTLSV1 and CTLSV5 fail to divide and form filaments. D. Cells expressing CTLSWT have a similar L/R ratio as wild type, which suggests that CTLSWT can support growth almost as well as wild type. Cells expressing CTLSV1 and CTLSV5 form long filaments with few Z-rings.

Discussion

The κ value of the CTL is the primary determinant of its function

A study of the native CTL variants shows that a κ close to that of wild type is necessary for proper FtsZ function. CTLV1, a low-κ variant, supports growth at the normal rate, but cells expressing it are longer, have fewer Z-rings, and degrade the FtsZ to a relatively small degree. CTLV5 and CTLV6, high-κ variants, caused significant growth defects and were degraded by the cells to a much greater degree. A study of the synthetic CTL variants shows that a κ value close to that of wild type is sufficient to support growth at almost the same rate as wild type. CTLSWT, which has the same κ as wild type supports growth almost as well as wild type, although there is some degradation in the cells. CTLSV1 and CTLSV5, extreme-κ synthetic CTL variants, do not support any growth, even if their cognate native CTL variant, as in the case of CTLSV1, supports growth. This discrepancy suggests that the κ value of the CTL may not be the only determinant of FtsZ function, but it is still probably the primary one.

The C-terminal linker of FtsZ is an intrinsically disordered peptide

The characteristics of the CTL, as found in this and previous studies, strongly implicate the CTL as an IDP. The dependence on κ for its functionality is a classic characteristic of polyampholytic IDPs, a class of proteins of which *B. subtilis* FtsZ is a member. As seen in Table 1, the CTL of *B. subtilis* FtsZ contains a substantial amount of charged residues, a fact also true for several other species in including *E. coli*. In species that have a polyampholytic CTL, the κ value of the CTL is well conserved around the value of the *B. subtilis* CTL (7). CTL sequences can be easily swapped between species as long as they are both polyampholytic of similar length (10). A polyampholytic CTL, however, cannot be replaced by an uncharged CTL, such as that of *Selenomonas ruminatium*, and still confer function to FtsZ (unpublished data).

The C-terminal linker of FtsZ is a flexible tether

It was first established in a previous study that the CTL is a flexible tether (10). The

dependence on the κ value of the CTL for the functionality of FtsZ alludes to its role in

determining flexibility. A high-κ IDP has segregated oppositely charged residues that causes the

peptide to fold into hairpin-like motifs, which would decrease the flexibility of the IDP. A low-κ

IDP has evenly distributed oppositely charged residues that cause the peptide to adopt a loose,

extended coiled conformation, which would be very flexible due to the lack of constraints on the

IDP. The fact that the κ value of the CTL must lie within a certain range for proper FtsZ function

suggests that there exists a range of flexibility within which the CTL must conform. A CTL with

a higher κ value than wild type is not flexible enough, but a CTL with a lower κ value than wild

type is too flexible. This parameter fits into the model of the CTL as a flexible tether between

FtsZ filaments and between the Z-ring and the membrane. A high-κ CTL may be too rigid to

support interactions between FtsZ filaments in the Z-ring, which must be a dynamic structure for

proper cell division. A low-κ CTL may be too loose to maintain Z-ring integrity or translate the

contraction of the Z-ring to the membrane.

The C-terminal linker of FtsZ as a target for antibiotics

FtsZ has long been recognized as a promising target for antibiotics. Overall, FtsZ is

widely conserved across many divisions of bacteria, which opens the possibility for FtsZ as a

target for broad-spectrum antibiotics. By targeting certain regions of FtsZ, however, an antibiotic

that targets FtsZ can be made more specific. PC190723 is a promising antibiotic that is most

effective against gram-positive bacteria (5). 297F is another drug that targets FtsZ and is most

effective against mycobacteria and shows no antibacterial activity against gram-positive or gram-

negative bacteria. Due to its low cytotoxicity, 297F has been proposed as a possible treatment for tuberculosis (14).

The CTL presents a unique opportunity due to its great variability between species. A drug that targets the CTL could, at least in theory, be species-specific. The lack of conformational consistency in the CTL might make the design of a drug targeting it difficult, but a study of α-synuclein, an IDP implicated in Parkinson's disease, has shown that IDPs can be targeted by drugs and that those drugs can have therapeutic effects (8). Such a drug would be tremendously beneficial in selectively targeting pathogenic bacteria while sparing commensal bacteria, thus limiting the spread of antibiotic resistance. In an age of alarmingly increasing rate of antibiotic resistance, discovering more antibiotics and using them more selectively are key in preventing post-antibiotic age.

Future Work

Many insights have been made into the CTL in recent years, but much remains to be discovered. A logical next step would be to replicate the *in vitro* experiments of the previous study (10). *In vitro* data could yield insight into how the κ value of the CTL is affecting FtsZ. It could be affecting FtsZ polymerization or bundling. GTPase assays allow the determination of the rate of FtsZ polymerization and the critical concentration. 90° light scattering assays allow the determination of the rate of FtsZ filament bundling and the strength of lateral interactions between FtsZ filaments. Electron microscopy allows the direct visualization of FtsZ polymers and Z-rings. Dynamic light scattering, a relatively new technique, can provide new information in addition to that provided by 90° light scattering: the length of FtsZ filaments and the rates of FtsZ polymerization and depolymerization (15).

Acknowledgements

I would like to thank PJ Buske for introducing me to this project and teaching me the experimental techniques in molecular microbiology and microbial genetics. I would like to thank Anuradha Mittal and Rohit Pappu for designing the CTL variant sequences in what has become a fruitful collaboration. I would like to thank Petra Anne Levin for outstanding mentorship, both in this project and in my undergraduate studies. I would like to thank all past and present members of the Levin lab for their help and support in learning techniques, troubleshooting, and creating a great work environment. Most of all, I would like to thank my mother for her unending support throughout my life in pursuing my dreams and goals.

References

(1) Bi EF, Lutkenhaus J. FtsZ ring structure associated with division in *Escherichia coli*. Nature. 1991 Nov 14; 354 (6349): 161-4.

(2) Erickson HP. Evolution of the cytoskeleton. Bioessays. 2007 Jul; 29 (7): 668-77.

(3) Levin PA, Losick R. Transcription Factor Spo0A switches the localization of the cell division protein FtsZ from a medial to a bipolar pattern in *Bacillus subtilis*. Genes & Development. 1996 Feb 15; 10 (4): 478-88.

(4) Weart RB, Lee AH, Chien AC, Haeusser DP, Hill NS, Levin PA. A metabolic sensor governing cell size in bacteria. Cell. 2007 Jul 27; 130 (2): 335-47.

(5) Erickson HP, Anderson DE, Osawa M. FtsZ in bacterial cytokinesis: cytoskeleton and force generator all in on. MMBR. 2010 Dec; 74 (4): 504-28.

(6) Arjes HA, Kriel A, Sorto NA, Shaw JT, Wang JD, Levin PA. Failsafe mechanisms couple division and DNA replication in bacteria. Current Biology. 2014 Sep 22; 24 (18): 2149-55.

(7) Buske PJ, Mittal A, Pappu RV, Levin PA. An intrinsically disordered linker plays a critical role in bacterial cell division. Seminars in Cell & Developmental Biology. 2015 Jan; 37C: 3-10.

(8) Toth G, Gardai SJ, Zago W, Bertoncini CW, Cremades N, Roy SL, Tambe MA, Rochet JC, Galvagnion C, Skibinski G, Finkbeiner S, Bova M, Regnstrom K, Chiou SS, Johnston J, Callaway K, Anderson JP, Jobling MF, Buell AK, Yednock TA, Knowles TP, Vendruscolo M, Christodoulou J, Dobson CM, Schenk D, McConlogue L. Targeting the intrinsically disordered structural ensemble of α-synuclein by small molecules as a potential therapeutic strategy for Parkinson's disease. PLoS One. 2014 Feb 14; 9 (2):

e87133.

(9) Buske PJ, Levin PA. Extreme C terminus of bacterial cytoskeletal protein FtsZ plays

fundamental role in assembly independent of modulatory proteins. Journal of Biological

Chemistry. 2012 Mar 30; 287 (14): 10945-57.

(10) Buske PJ, Levin PA. A flexible C-terminal linker is required for proper FtsZ assembly *in*

vitro and cytokinetic ring formation *in vivo*. Molecular Microbiology. 2013 Jul; 89 (2):

249-63.

(11) Weart RB, Levin PA. Growth rate-dependent regulation of medial FtsZ ring formation.

Journal of Bacteriology. 2003 May; 185 (9): 2826-34.

(12) Perego M, Spiegelman GB, Hoch JA. Structure of the gene for the transition state regulator,

abrB: regulator synthesis is controlled by the spo0A sporulation gene in *Bacillus subtilis*.

Molecular Microbiology. 1988 Nov; 2 (6): 689-99.

(13) Ireton K, Rudner DZ, Siranosian KJ, Grossman AD. Integration of multiple developmental

signals in *Bacillus subtilis* through the Spo0A transcription factor. Genes &

Development. 1993 Feb; 7 (2): 283-94.

(14) Lin Y, Zhu N, Han Y, Jiang J, Si S. Identification of anti-tuberculosis agents that target the

cell-division protein FtsZ. Journal of Antibiotics (Tokyo). 2014 Sep; 67 (9): 671-6.

(15) Hou S, Wieczorek SA, Kaminski TS, Ziebacz N, Tabaka M, Sorto NA, Foss MH, Shaw JT,

Thanbichler M, Weibel DB, Nieznanski K, Holyst R, Garstecki P. Characterization of

Caulobacter crescentus FtsZ protein using dynamic light scattering. Journal of Biological

Chemistry. 2012 Jul 6; 287 (28): 23878-86.